



**EUROfusion**

WPHCD-PR(18) 20694

R Agnello et al.

**Cavity Ring Down Spectroscopy to  
measure negative ion density in a  
helicon plasma source for fusion neutral  
beams**

Preprint of Paper to be submitted for publication in  
Review of Scientific Instruments



This work has been carried out within the framework of the EUROfusion Consortium and has received funding from the Euratom research and training programme 2014-2018 under grant agreement No 633053. The views and opinions expressed herein do not necessarily reflect those of the European Commission.

This document is intended for publication in the open literature. It is made available on the clear understanding that it may not be further circulated and extracts or references may not be published prior to publication of the original when applicable, or without the consent of the Publications Officer, EUROfusion Programme Management Unit, Culham Science Centre, Abingdon, Oxon, OX14 3DB, UK or e-mail [Publications.Officer@euro-fusion.org](mailto:Publications.Officer@euro-fusion.org)

Enquiries about Copyright and reproduction should be addressed to the Publications Officer, EUROfusion Programme Management Unit, Culham Science Centre, Abingdon, Oxon, OX14 3DB, UK or e-mail [Publications.Officer@euro-fusion.org](mailto:Publications.Officer@euro-fusion.org)

The contents of this preprint and all other EUROfusion Preprints, Reports and Conference Papers are available to view online free at <http://www.euro-fusionscipub.org>. This site has full search facilities and e-mail alert options. In the JET specific papers the diagrams contained within the PDFs on this site are hyperlinked

# Cavity Ring-Down Spectroscopy to measure negative ion density in a helicon plasma source for fusion neutral beams

R. Agnello,<sup>1</sup> M. Barbisan,<sup>2,3</sup> I. Furno,<sup>1</sup> Ph. Guittienne,<sup>4</sup> A.A. Howling,<sup>1</sup> R. Jacquier,<sup>1</sup> R. Pasqualotto,<sup>2</sup> G. Plyushchev,<sup>1</sup> Y. Andrebe,<sup>1</sup> S. Béchu,<sup>5</sup> I. Morgal,<sup>6</sup> and A. Simonin<sup>6</sup>

<sup>1</sup>*Ecole Polytechnique Fédérale de Lausanne (EPFL), Swiss Plasma Center (SPC), CH-1015 Lausanne, Switzerland*

<sup>2</sup>*Consorzio RFX, Corso Stati Uniti 4, I-35127 Padova, Italy*

<sup>3</sup>*INFN-LNL, v.le dell'Università 2, I-35020, Legnaro, Italy*

<sup>4</sup>*Helyssen, Route de la Louche 31, CH-1092 Belmont-sur-Lausanne, Switzerland*

<sup>5</sup>*Université Grenoble-Alpes, CNRS, Grenoble INP, LPSC-INP23, 38000 Grenoble, France*

<sup>6</sup>*CEA, IRFM, F-13108 St-Paul-lez-Durance, France*

(Dated: 8 June 2018)

Cavity Ring Down Spectroscopy (CRDS) is used to measure the  $D^-$  absolute density produced in the helicon plasma reactor RAID (Resonant Antenna Ion Device) at the Swiss Plasma Center. The bird-cage geometry of the helicon antenna produces a homogeneous, high-density plasma column ( $n_e = 1.5 \times 10^{18} \text{ m}^{-3}$  in  $H_2$  at 0.3 Pa and 3 kW of input power) 1.4 m long. We present the CRDS experimental setup, its positioning on the RAID reactor and how the mechanical and thermal effects of the plasma affect the measurement. First results in deuterium plasma confirm a production of negative ions ( $D^-$ ) with a significant density: an average value of  $3.0 \times 10^{16} \text{ m}^{-3}$  of  $D^-$  is obtained at 0.3 Pa and 5 kW of power input in Cs-free plasma. This result is in good agreement with calculations performed with the collisional radiative code YACORA.

## I. INTRODUCTION

Neutral Beam Injectors (NBIs) for future fusion devices will be based on negative deuterium ions and will have to fulfill high standards in terms of spatial uniformity, CW operation, and beam minimal co-extracted electron current. For example, the NB designed for DEMO will have to provide an energy of 800 keV and a current of 34 A.<sup>1</sup> Furthermore, in a prospective fusion power plant, reducing the cost of the electricity will pose severe constraints on the wall-plug efficiency ( $> 50\%$ ) and RAMI (reliability, availability, maintainability and inspectability) aspects of the overall NBI system. In the present DEMO conceptual design, a modular system is proposed in which plasma is produced by 20 inductively-coupled plasma (ICP) sources, each requiring more than 90 kW of radiofrequency (RF) power.<sup>2</sup> Negative ions are dominantly generated as a result of the interaction of a neutral deuterium atom (D) or ion ( $D^+$ ) with a caesiated surface (the so-called surface production process). The negative ion beam is formed by two blade-shape apertures with a large height and small width to optimize the vacuum conductance, reducing stripping losses. This concept is also compatible with the adoption of a photo-neutralizer system with higher efficiency than gas-based neutralizers.<sup>3</sup>

The possibility of using helicon plasma discharges as negative ion sources for fusion NBIs has been suggested<sup>4</sup> and is presently explored in the framework of the EUROfusion work package on heating and current drive (WPHCD) within the Power Plant Physics and Technology Project.<sup>12</sup> Helicon sources may have several advantages over traditional ICP generators: 1) lower required RF power, leading to wider operational domain

and high electron density; 2) stable operation at low pressure ( $< 0.3$  Pa) resulting in reduced negative ion losses by electron stripping; 3) higher efficiency of negative ion production in volume production mode, and a high degree of molecular dissociation, which would be favorable in a caesiated source; and 4) by producing a magnetized plasma column, they are well-adapted to a blade-shape geometry. However, the physics and technical challenges of helicon-based negative ion sources for fusion are still largely unexplored today.

The Resonant Antenna Ion Device (RAID) at the Swiss Plasma Center is a prototype helicon plasma source for NBs, where steady state plasma discharges produced by an RF antenna in a bird-cage geometry<sup>13</sup> in different gases such as  $H_2$ ,  $D_2$ , Ar and He are investigated. Previous experimental campaigns performed on RAID, using optical emission spectroscopy (OES), showed promising results in terms degree of dissociation and favorable scaling with injected RF power.<sup>11</sup> OES provides indirect measurements of the negative ion density and degree of dissociation. Since it requires the interpretation of spectral line measurements by means of the collisional radiative code YACORA,<sup>14</sup> a direct measurement of negative ion density, based on a different physical mechanism, is then necessary to confirm past observations and to have a more reliable analysis of negative ion production.

Two techniques can be used: 1) Langmuir Probe (LP) laser photodetachment;<sup>19</sup> and 2) Cavity Ring-Down Spectroscopy.<sup>18</sup> The former has been successfully applied in the MAGPIE helicon plasma device showing densities up to  $6 \times 10^{15} \text{ m}^{-3}$ .<sup>8</sup> The main problem of using LP photodetachment is that it requires the measurement of the local electron density which is hard to determine accurately with LPs since they locally

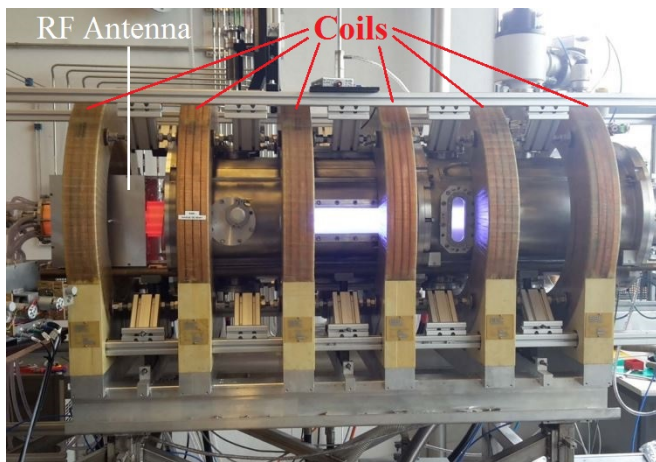


FIG. 1. A picture of the RAID plasma device. The cylindrical vacuum vessel is surrounded by six coils producing an axial magnetic field up to 800 G. The resonant antenna is inside the aluminium Faraday cage surrounded by the first coil on the left.

perturb the plasma and furthermore they cannot be used in the high power continuous operation, such as in RAID.

CRDS is also based on the laser photodetachment but does not need a LP, it is a direct and non-invasive technique that can be used to measure the line-integrated density of negative ions in plasmas. CRDS has already been applied in the fusion community to measure the line integrated  $H^-/D^-$  density in various inductive plasma sources.<sup>6,7,9</sup> Up to now, however, no CRDS measurement has been performed in a  $H_2$  or  $D_2$  helicon plasma.

The paper is structured as follows: in section II, the description of the RAID device is presented. Section III introduces the CRDS technique and its application to negative ions for fusion, the details of the implementation of the experimental set up in RAID and the tests in vacuum and gas. Section IV discusses the preliminary results in a deuterium plasma and, in conclusions, further developments are presented.

## II. THE RESONANT ANTENNA ION DEVICE (RAID)

RAID produces a magnetized plasma column by helicon wave excitation.<sup>12</sup> A picture of RAID is shown in Fig. 1. The vacuum chamber has a 0.4 m internal diameter and 1.40 m length. Plasmas are sustained by a 10 kW birdcage-geometry RF resonant antenna<sup>13</sup> operating at 13.56 MHz. Many gases can be used such as  $H_2$ ,  $D_2$ , Ar and He and typical electron densities of  $10^{18} m^{-3}$  and  $10^{19} m^{-3}$ , respectively, in hydrogen and argon can be attained. The pressure is controlled by mass flow controllers at a constant turbo pumping speed of 170 l/s. A pressure of 0.3 Pa is normally used as required in DEMO to minimize the ion losses due to collisions with the gas molecules in the NB system.<sup>1</sup> The vessel is surrounded

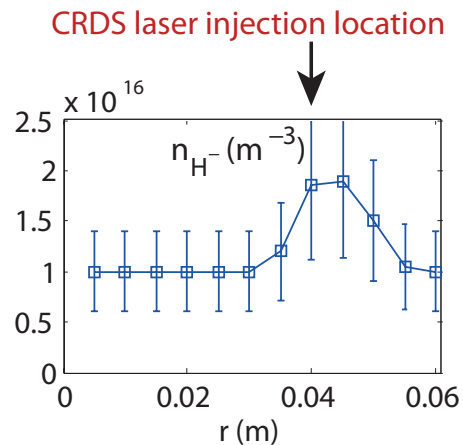


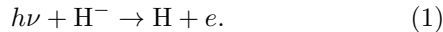
FIG. 2. Radial distribution of  $n_{H^-}$  as measured by OES at 1.0 m from the RF antenna: the density is peaked off-axis.

by copper coils producing an on-axis magnetic field up to 800 G. The polarity of the first coil can be reversed to create a divergent magnetic field at the antenna position, this is to facilitate plasma ignition. The plasma column deposits part of its energy on the water-cooled copper plate which is placed at the end of the vessel and can be arbitrarily polarized to study different plasma confinement configurations. As shown by microwave interferometry measurements, the electron density in  $H_2$  and  $D_2$  with 3 kW injected power reaches  $1.5 \times 10^{18} m^{-3}$  on the axis of the plasma column and has a good homogeneity along the axial direction.<sup>12</sup> Previous OES measurements revealed a significant volume production of  $H^-$ . Their radial distribution is shown in Fig. 2.<sup>11</sup> and suggests that negative ions reach a maximum density in a radial shell located around  $r \sim 4$  cm. This radial shell is the region sampled by the CRDS, as discussed in the next section.

## III. THE CRDS EXPERIMENTAL SETUP AND FIRST TESTS IN VACUUM AND GAS

CRDS is a technique introduced by O'Keefe in 1988 to measure absorption spectra.<sup>5</sup> The main features of CRDS is that it is very sensitive, directly measures the number density and is independent of the intensity of the light source. The main element of a CRDS system is an optical cavity made of two very high reflectivity (HR) mirrors between which the light undergoes multiple reflections thus multiplying the interaction length of the light with the absorbing medium. CRDS can be applied as a plasma diagnostics to measure the number density of different plasma species. Particularly relevant in the field of fusion is its application for the measurement of  $H^-$  and  $D^-$  in negative ion sources for neutral beams.<sup>6,7,15</sup> In this case, the employed light source is usually a Nd:YAG laser whose photon energy ( $E = 1.2$  eV, corresponding to a wavelength of  $\lambda = 1064$  nm) is enough to strip the weakly

bound electron of  $\text{H}^-$  and  $\text{D}^-$  ( $E_{\text{binding}} = 0.75 \text{ eV}$ ) by photodetachment:



The light reflected back and forth inside the cavity is lost both because of the transmission of the mirrors and of the presence of an absorbing medium along the line of sight (LOS) of the laser. The signal leaking through the cavity shows an exponential decay according to:

$$I(t) = I_0 e^{-t/\tau}, \quad (2)$$

where  $I_0$  is the initial intensity, and  $\tau$ , the time it takes to reduce  $I_0$  by a factor  $e$ , is given by:

$$\tau = \frac{L}{c(1 - R + \alpha d)}, \quad (3)$$

where  $L$  is the cavity length,  $c$  the speed of light,  $R$  the reflectivity of the mirrors, and  $\alpha$  is the absorption coefficient.  $\alpha$  is given by  $\bar{n}_{\text{H}^-} \sigma_{\text{H}^-}$ , where  $\sigma_{\text{H}^-}$  is the interaction cross section ( $\sigma_{\text{H}^-} = 3.5 \times 10^{-21} \text{ m}^2$  at a wavelength of  $1064 \text{ nm}$ <sup>19</sup>) and  $\bar{n}_{\text{H}^-}$  is the  $\text{H}^-$  line-integrated density.  $d$  is the path length of the laser beam in the absorbing medium and is usually the parameter more affected by uncertainty. Eq. 3 can be inverted to obtain  $\bar{n}_{\text{H}^-}$

$$\bar{n}_{\text{H}^-} = \frac{1}{\sigma_{\text{H}^-}} \frac{L}{cd} \left( \frac{1}{\tau} - \frac{1}{\tau_0} \right), \quad (4)$$

where  $\tau_0$  is the decay time without plasma, and  $\tau$  in the presence of plasma.

Fig. 3(a) shows a side view of RAID and the position where the Nd:YAG laser beam is injected into the vacuum vessel. As shown in Fig. 3(b) the LOS of the laser is perpendicular to the axis of the plasma column and passes at a radial distance of  $0.04 \text{ m}$  from the axis: in this position a higher concentration of negative ions is expected, according to the OES measurements in Fig. 2. We estimate an effective negative ion chord length  $d \sim 0.05 \text{ m}$  given by the intersection of the laser beam and a negative ion shell of  $0.035 \text{ m}$  internal radius and  $0.015 \text{ m}$  width.

The Nd:YAG laser beam has a diameter of  $6 \text{ mm}$ , divergence  $< 0.7 \text{ mrad}$  and FWHM pulse duration of  $\Delta t \simeq 5 \text{ ns}$ . This last parameter determines the minimum length  $L_{\text{min}} = c\Delta t/2 = 0.75 \text{ m}$  of the cavity to avoid overlapping modes. As shown in Fig. 3 two tube extensions are employed to obtain a cavity length  $L = 0.91 \text{ m}$ .

The optical stability of the cavity is provided by the radius of curvature  $r$  of the mirrors from the condition  $r > L/2$ .<sup>16</sup> Two Layertech HR mirrors with nominal reflectivity  $R = 99.994\%$  and radius of curvature  $r = 1 \text{ m}$  are employed.<sup>17</sup> The HR mirrors can be finely tilted by

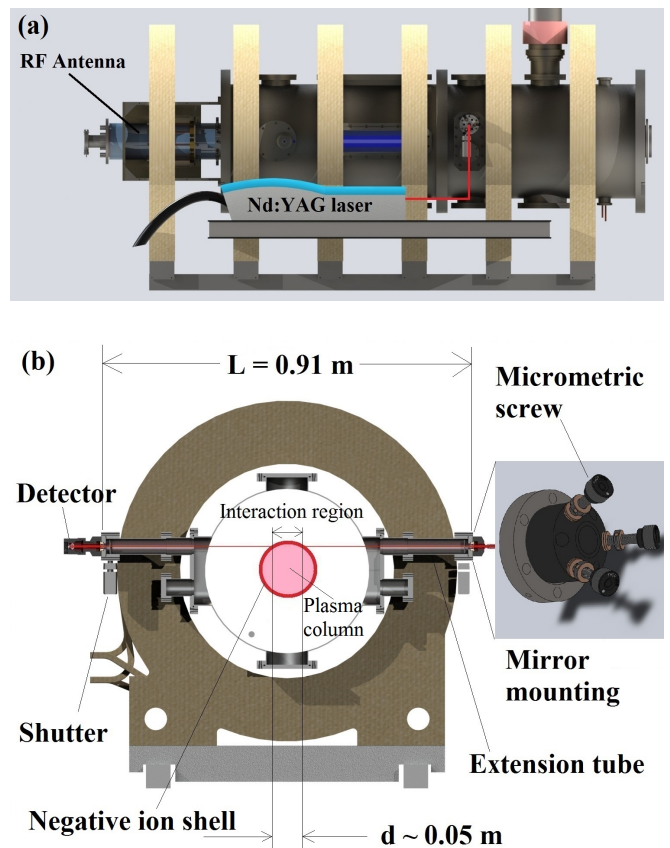


FIG. 3. (a) Side view of RAID: the laser beam is steered and enters the optical cavity installed in the vessel perpendicularly to the RAID axis.

(b) Transversal section of RAID in the plane of the the CRDS: the LOS of the laser beam (schematically shown in red) is displaced from the plasma column center by  $4 \text{ cm}$  so that it passes through the  $\text{H}^-/\text{D}^-$  shell.

means of three micrometric screws on the mirror mounting, (inset in Fig. 3(b)), to perform the alignment of the laser beam inside the optical cavity. The mirrors' reflectivity is the parameter that determines the sensitivity of the experimental set up. Before installation of HR mirrors on RAID, their reflectivity was measured on a testbench consisting of a  $1.8 \text{ m}$  long cavity. A reflectivity of  $R = 99.9953\%$  was measured, employing Eq. 3 in vacuum, confirming the nominal reflectivity.

The reflectivity of the mirrors must be kept as high as possible: the minimum detectable density indeed depends on this parameter. To limit the exposure time of the mirrors to the plasma environment, a mechanical shutter in each extension is closed when the CRDS is not operational (see Fig. 3(b)). Moreover, to reduce the effect of incoming energetic particles impacting on the mirror HR coating, the feeding gas is flushed in front of the HR mirrors.

The laser light transmitted through the far-side mirror is collected by a photodiode detector after having been focused by a lens. The photodiode has a  $3 \text{ mm}$  diameter

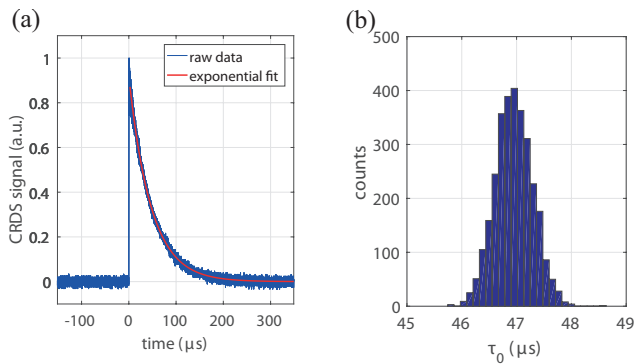


FIG. 4. (a) A typical decay signal measured in vacuum at the photodiode detector: the laser pulse (pulse energy 65 mJ) strikes the detector at  $t = 0$ . The decay constant  $\tau_0$  is calculated from the exponential fit (red continuous line). (b) The histogram shows the distribution of  $\tau_0$  over 3000 laser shots. The standard deviation  $\sigma_{\tau_0}$  of the distribution determines the sensitivity of the CRDS diagnostic.

active area, internal gain 75, transimpedance amplifier  $4 \times 10^3 V/A$  and 40 MHz bandwidth.<sup>10</sup> The signal is then acquired by a waveform recorder LeCroy 755Zi with 10 MS/s sampling rate and 14 bit digitization in a time window of 1 ms. The laser was pulsed at a frequency of 10 Hz, i.e. 10 ring down signals per second; this was seen to be a good trade off between the temporal fluctuation of  $\tau_0$  and the data acquisition rate.

A typical decay signal in vacuum measured at the detector is shown in Fig. 4(a). The initial transient peak at time  $t = 0$  s corresponds to the instant at which a laser pulse strikes the mirror in front of the detector for the first time. After a few reflections, the transversal modes are damped and only the Gaussian mode survives in the optical cavity. The calculation of  $\tau_0$  is performed by an exponential fit (in red in Fig. 4(a)) after the first two microseconds of the signal, to exclude by the cavity transient undamped modes. An average  $\tau_0$  of  $46.95 \mu\text{s}$  with a standard deviation  $\sigma_{\tau_0}$  of  $0.34 \mu\text{s}$  was found (baseline noise of 0.7%) for 3000 shots as shown in Fig. 4(b). This corresponds to a reflectivity  $R = 99.9935\%$ , which is slightly smaller (-0.0005%) than the nominal one. The reason for this loss of reflectivity might be due to dust deposition on mirrors surfaces during the installation on RAID. The error on the exponential fit was of the order of 0.1%. The time fluctuation of  $\tau_0$ , being much bigger than the error on the fit, can be used to estimate the lowest detectable density for a single measurement of  $H^-/D^-$  in RAID and it results in  $\bar{n}_{min} = (1-R) \frac{1}{\sigma_{D^-} d} \frac{\sigma_{\tau_0}}{\tau_0} \sim 2.7 \times 10^{15} \text{ m}^{-3}$ . This lower limit can be decreased by a factor  $\sqrt{N}$  by averaging over  $N$  CRDS signals.

The alignment of laser beam with the axis of the optical cavity is crucial. If the beam enters misaligned with respect to the optical cavity the ringdown time can vary strongly. Thus, an iterative adaptive procedure was adopted to stabilize the  $\tau$  level. This, combined with mechanical vibrations of the rotary-pumps and of the ves-

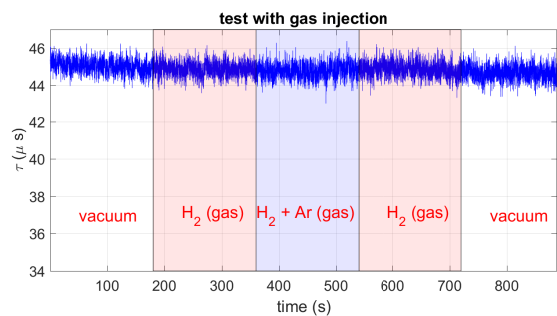


FIG. 5. The picture shows the trend of  $\tau$  during different gas injections demonstrating that the optical cavity is not perturbed by different gas flushing.

sel water cooling and thermal effects due to the plasma, make CRDS a challenging diagnostic in this scenario. To check if the gas flushing induced a mechanical stress on the optical cavity ( $H_2/D_2$  are flushed through the mirror mountings) the temporal behavior of  $\tau$  for different pressure conditions was studied. Fig. 5 shows the  $\tau$  evolution in vacuum, in  $H_2$  gas at 0.35 Pa and in a mixture of  $H_2 + Ar$  gas at 0.74 Pa. As shown,  $\tau$  remains stable during the entire phase. This is a proof that perturbation due to the gas flushing can be neglected during different gas injection phases.  $\tau$  in these tests is slightly less than in vacuum (by  $\sim 2.0 \mu\text{s}$ ). This is maybe due to a loss of alignment or dust deposition on mirrors caused by gas flushing.

#### IV. FIRST RESULTS IN A $D_2$ PLASMA

The measurements in plasma were performed with  $H_2$ ,  $D_2$  and Ar plasmas at a constant pressure of 0.3 Pa and a magnetic field of 200 G to make them comparable with past OES measurements.<sup>11</sup>

The technique consists in measuring the  $\tau$  before, during, and after a plasma discharge. A typical  $\tau$  measurement in a  $D_2$  plasma at 5 kW RF power and with an argon plasma at 700 W RF power are respectively shown in Fig. 6(a) and 6(b). The RF power in argon was limited at 700 W because of sputter damage on HR mirrors coating.

In Fig. 6(a), during the first 300 s only  $D_2$  gas is present and the RF power is off. Argon gas is injected to facilitate plasma ignition a few seconds before it. At  $t = 300$  s the plasma discharge is initiated and the argon gas flow is stopped. This transient time when there is a mixture of  $D_2$  and Ar plasma lasts about 50 s. During this time the power of the discharge is increased while the system automatically matches the impedance to minimize the reflected RF power. During this period (50 s), the  $\tau$  decrease is due to the combination of  $D^-$  absorption and a thermal effect on the cavity. After  $t = 350$  s, only  $D_2$  is injected and maintained stable for about 150 s. Then, the plasma is turned off at  $t = 500$  s and  $\tau$  exhibits a

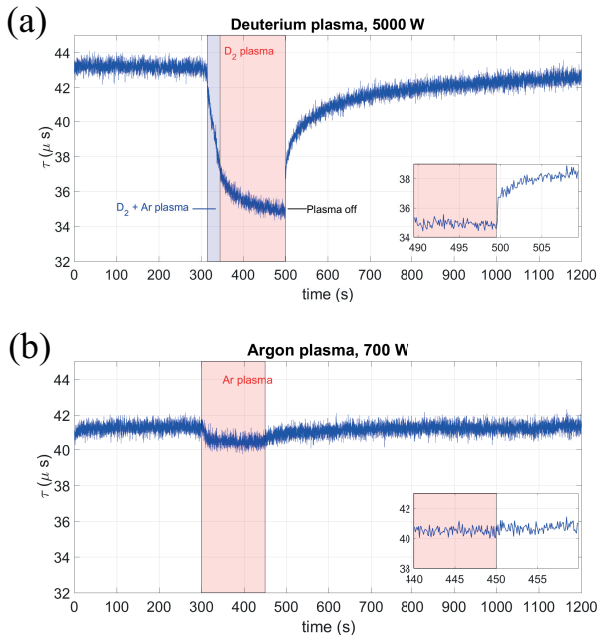
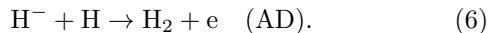
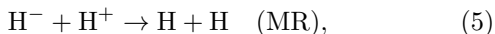


FIG. 6. The time evolution of  $\tau$  before, during and after the plasma discharge for a  $D_2$  plasma (a) and for an Ar plasma (b) at a pressure of 0.3 Pa. The red area identifies when the plasma is on. The box inset is a zoom around the instant when the plasma is turned off ( $t = 500$  s for  $D_2$ , and  $t = 450$  s for Ar). The  $D_2$  exhibits a jump due to  $D^-$  disappearance (see zoombox in (a)), while no jump is observed for the Ar plasma (see zoombox in (b)).

jump from  $34.8 \mu\text{s}$  to  $37.1 \mu\text{s}$  between two consecutive acquisitions (see zoom box at  $t = 500$  s in Fig. 6(a)) due to the sudden disappearance of the  $D^-$ .

A few considerations will be presented in the next lines to discuss how  $D^-$  ions are lost; we will take into account the case of  $H^-$  for this purpose but it remains valid for the  $D^-$ . In the energy range of RAID plasma, the typical  $H^-$  temperature is  $\sim 0.1$  eV. At this energy the processes that play the most important role in  $D^-$  destruction are mutual neutralization (MN) and associative detachment (AD),<sup>20</sup> respectively described by the Eqs. 5 and 6:



An estimation of the characteristic loss times of  $H^-$  for MR and AD processes are given by:  $t_{MR} \sim 1/(n_{H^+}\sigma_{MR}v_{RM})$  and  $t_{AD} \sim 1/(n_H\sigma_{AD}v_{AD})$  where  $v_{RM}$  and  $v_{AD}$  are the center of mass velocities and  $n_H$  is the density of H. The cross section for the MR,  $\sigma_{MR}$ , at 0.1 eV is about  $2 \times 10^{-13} \text{ cm}^2$ .<sup>20</sup> The cross section for the AD,  $\sigma_{AD}$ , at the same energy,<sup>20</sup> is two orders of magnitude smaller than  $\sigma_{MR}$  however, the H density in the  $D^-$  shell is about two or three orders of magnitude higher

than  $n_{D^-}$  as shown by OES measurements.<sup>11</sup> For both MR and AD processes, the estimation of the characteristic loss time  $t_{MR,AD}$  of  $D^-$  is in the order of  $\sim 0.1$  ms which is much less than the time between two consecutive CRDS acquisitions (100 ms).

As one can clearly see in Fig. 6(a), together with the rapid jump due to the plasma extinction, there is also a slower variation, lasting some minutes after the plasma is turned off. The  $\tau$  takes more than ten minutes to recover to its initial value before the plasma discharge. Even during the plasma  $D_2$  discharge,  $\tau$  has a drift. These long period drifts are mostly likely due to thermal effects causing a distortion of the optical cavity.

In order to be sure that the sudden jump is solely due to the disappearance of negative ions, a test with an argon plasma, not contributing to laser absorption, was performed. No jump occurred when the argon plasma was turned off (see zoom box in Fig. 6(b)), confirming that the jump seen in  $D_2$  plasma is solely due to the disappearance of negative ions produced in this plasma. A gradual drop  $\delta\tau$  of about  $0.5 \mu\text{s}$ , at the limit of the sensitivity, is observed when the argon plasma is turned on. This is due to a loss of alignment caused by the thermal expansion of the cavity. When the argon plasma is turned off,  $\tau$  recovers slowly to its pre-discharge value after some minutes.

Thus, the fast dynamics that characterizes the plasma extinction, with respect to the slow drift of optical cavity thermal expansion, can be taken as a signature of the negative ion disappearance in  $H_2$  and  $D_2$  plasmas. By making a linear fit of  $\tau$  a few seconds before and after the  $\tau$  jump (from  $34.8$  to  $37.1 \mu\text{s}$ ), the  $D^-$  density can be calculated. The error on the calculation of  $\bar{n}_{D^-}$  is given by the errors on the coefficients of the linear fit. An average density  $\bar{n}_{D^-}$  on a 5 cm path length of  $(3.045 \pm 0.085) \times 10^{16} \text{ m}^{-3}$  is deduced; this value is comparable to the results of OES in Fig. 2.

## V. CONCLUSIONS

A CRDS diagnostic has been installed and successfully employed on the RAID device to measure  $D^-$  density providing results in agreement with previous OES measurements. We showed that  $D^-$  is produced in the volume of a steady state Cs-free helicon plasma discharge with a line-integrated average density of  $\bar{n}_{D^-} = (3.045 \pm 0.085) \times 10^{16} \text{ m}^{-3}$ . The filling gas pressure was 0.3 Pa, which is the operational pressure of negative ion sources for fusion and, the RF input power was 5 kW. Various technical aspects were investigated during this preliminary measurement campaign, such as the implementation of the experimental setup and the thermal effects on the optical cavity caused by the plasma discharge. The dependence of the ringdown time on the precise mirror alignment in presence of mechanical vibrations and thermal distortion in presence of plasma, combined with a critical sensitivity to mirror reflectivity,

makes CRDS a challenging diagnostic in this scenario. A further CRDS experimental campaign is planned where the dependence of  $H^- / D^-$  formation on different plasma conditions like input power and gas pressure will be explored.

## ACKNOWLEDGMENTS

This work has been carried out within the framework of EUROfusion Consortium and has received funding from the Euratom research and training program 2014-2018 under grant agreement No 633053. The views and opinions expressed herein do not necessarily reflect those of the European commission. We gratefully acknowledge the mechanical and electronic workshops of the Swiss Plasma Center for their constant support. We thank Maurizio Giacomini for the useful discussions on reactions cross sections in plasmas.

- <sup>1</sup>P. Sonato, P. Agostinetti, T. Bolzonella, F. Cismondi, U. Fantz, A. Fassina, T. Franke, I. Furno, C. Hopf, and I. Jenkins, *Nucl. Fusion* **57**, 056026 (2017).
- <sup>2</sup>U. Fantz, C. Hopf, D. Wunderlich, R. Friedl, M. Fröschle, B. Heinemann, W. Kraus, U. Kurutz, R. Nocentini and L. Schiesko, *Nucl. Fusion* **57**, 116007 (2017).
- <sup>3</sup>A. Simonin, R. Agnello, S. Bechu, J. M. Bernard, C. Blondel, J. P. Boeuf, D. Bresteau, G. Cartry, W. Chaibi, and C. Drag, *New J. Phys.* **18**, 125005 (2017).
- <sup>4</sup>S. Briefi and U. Fantz, *AIP Conference Proceedings*, **1515**, 278 (2013).
- <sup>5</sup>A. O’Keefe and D. G. Deacon, *Rev. Sci. Instrum.* **59**, 2455 (1988).
- <sup>6</sup>H. Nakano, K. Tsumori, M. Shibuya, S. Geng, M. Kasaki, K. Ikeda, K. Nagaoka, M. Osakabe, Y. Takeiri and O.Kaneko, IOP publishing, 17th International Symposium on Laser-Aided Plasma Diagnostics, (2015).
- <sup>7</sup>M. Berger, U. Fantz, S. Christ-Koch and NNBI Team, *Plasma Sources Sci. Tech.* **18**, 025004 (2009).
- <sup>8</sup>J. Santos, R. Manoharan, S, O’Byrne and C. S. Corr, *Phys. Plasmas* **22**, 093513 (2015).
- <sup>9</sup>S. Cristofaro, R. Friedl and U. Fantz, *AIP Conference Proceedings* **1869**, 030036 (2017).
- <sup>10</sup>R. Pasqualotto, P. Nielsen and L. Giudicotti, *Rev. Sci. Instrum.* Vol. **72**, No. 1 (2001).
- <sup>11</sup>C. Marini, R. Agnello, B. P. Duval, I. Furno, A. A. Howling, R. Jacquier, A. N. Karpushov, G. Plyushchev, K. Verhaegh, and Ph. Guittienne, *Nucl. Fusion* **57**, 036024 (2017).
- <sup>12</sup>I. Furno, R. Agnello, U. Fantz, A.A. Howling, R. Jacquier, C. Marini, G. Plyushchev, Ph. Guittienne, and A. Simonin, *EPJ Web of Conferences* **157**, 03014 (2017).
- <sup>13</sup>P. Guittienne and E. Chavalier, *J. of Appl. Phys.* **98**, 083304 (2005).
- <sup>14</sup>Wunderlich D., Dietrich S. and Fantz, *J. Quant. Spectrosc. Radiat. Transfer* **110**, 62-71 (2009).
- <sup>15</sup>R. Pasqualotto, A. Alfier and L. Lotto, *Rev. Sci. Instrum.* **81**, 10D710 (2010).
- <sup>16</sup>Bahaa E. A. Saleh, Malvin Carl Teich, *Fundamentals of Photonics*, John Wiley and Sons, Inc. (1991).
- <sup>17</sup><https://www.layertec.com>, LAYERTEC GmbH website.
- <sup>18</sup>F. Grangeon, C. Monard, J.L. Dorier, A. A. Howling, Ch. Hollenstein, D. Romanini and N. Sadeghi, *Plasma Sources Sci. T.* **8**, 448 (1999).
- <sup>19</sup>M. Bacal, *Rev. Sci. Instrum.* **71**, 3981 (2000).
- <sup>20</sup>A. Spyridon, *Experimental Study of  $H^-$  negative ion production by electron cyclotron resonance plasmas*, Université Grenoble Alpes, (2016).